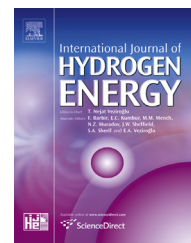


Available online at www.sciencedirect.com

ScienceDirect

journal homepage: www.elsevier.com/locate/ijhydene

Hydrogen insertion in substoichiometric titanium carbide



Julien Nguyen, Nicolas Glandut, Cédric Jaoul, Pierre Lefort*

Science des Procédés Céramiques et de Traitements de Surface (SPCTS), UMR 7315, CNRS, University of Limoges, European Ceramics Center, 12 Rue Atlantis, 87068 Limoges, France

ARTICLE INFO

Article history:

Received 4 February 2015

Received in revised form

29 April 2015

Accepted 1 May 2015

Available online 26 May 2015

Keywords:

Titanium carbide

Hydrogen storage

Vacancy ordering

Electrochemical insertion

ABSTRACT

Titanium carbide allows the insertion of hydrogen inside its structure, but only under two conditions. First, the carbide must be as substoichiometric as possible, i.e. close to $\text{TiC}_{0.60}$, because hydrogen requires the presence of carbon vacancies to penetrate the carbide. Second, the carbon vacancies must be ordered, leaving the (111) planes as empty as possible. The corresponding ordered structure is trigonal (space group R-3m). The other carbide structures (disordered Fm-3m NaCl type, or ordered Fd-3m) allow only little hydrogen insertion. Experimentally, samples of different stoichiometries were tested; they were obtained by reactive sintering of mixtures $\text{TiC}_{0.98} + \text{Ti}$ at 2100 °C, which gave the disordered structure Fm-3m. The trigonal structure was obtained from the disordered one, utilising a 40 h annealing treatment in argon at 730 °C. Longer treatments favored the structure Fd-3m. Hydrogen was inserted electrochemically, but other methods to achieve this result could exist. The interest of substoichiometric TiC_x lies in its low density, its chemical inertia and its cost, cheaper than noble metals.

Copyright © 2015, Hydrogen Energy Publications, LLC. Published by Elsevier Ltd. All rights reserved.

Introduction

Titanium carbide is a well known ceramic material [1,2]. The cubic phase TiC_x , exhibits a very wide composition range, from $\text{TiC}_{0.55}$ to $\text{TiC}_{0.98}$, in the titanium–carbon binary phase diagram [3]. The storage of hydrogen in this material has been considered for long, but mainly in very porous layers [4].

Now, it has been shown that hydrogen can be inserted electrochemically into hot-pressed substoichiometric titanium carbide (bulk), but this insertion depends on the stoichiometry of the carbide: the hydrogen storage capacity reached 2.9 wt. % into $\text{TiC}_{0.60}$, while $\text{TiC}_{0.90}$ did not allow any hydrogen insertion [5]. First-principles calculations [6] have

confirmed the ability of substoichiometric titanium carbide to store hydrogen.

A recent study showed that the long-range ordering of carbon vacancies in $\text{TiC}_{0.60}$ is responsible for electrochemical hydrogen insertion, which is only possible when this carbide has the trigonal superstructure, of space group R-3m [7]. Indeed, this structure contains alternately empty and full (111) carbon atomic planes and it was considered that the (111) empty planes constituted excellent paths for the diffusion of hydrogen into the structure [8–11]. Hydrogen diffusivity in the R-3m $\text{TiC}_{0.60}$ phase has been estimated at ca. $1.2 \times 10^{-13} \text{ cm}^2 \text{ s}^{-1}$.

For a better understanding of the insertion mechanism into titanium carbide, it was now necessary to couple the

* Corresponding author.

E-mail address: pierre.lefort@unilim.fr (P. Lefort).

<http://dx.doi.org/10.1016/j.ijhydene.2015.05.009>

0360-3199/Copyright © 2015, Hydrogen Energy Publications, LLC. Published by Elsevier Ltd. All rights reserved.

structural study of this material with the search of its ability for hydrogen storage. On these bases, and within the development of new materials for energy storage and conversion, the present study was devoted to the carbide TiC_x ability to store hydrogen in its whole stoichiometry field ($0.55 \leq x \leq 0.98$).

Material and methods

Samples preparation

TiC_x samples were prepared from mixtures of titanium carbide and titanium metal according to:



Titanium metal powder (purity 99.95%) was provided by Neyco, France. Titanium carbide powder (purity 99.5%, from Cerac Inc., USA), presented by the supplier as $\text{TiC}_{1.00}$, has been considered as composed of substoichiometric carbide $\text{TiC}_{0.98}$. The metal powder was micron-sized, with submicron particles, while the carbide was composed of slightly bigger grains (ca. 2 μm) with angular shapes, probably obtained by grinding of bigger lumps.

Different samples of compositions TiC_x , with $x = 0.55; 0.60; 0.65; 0.70; 0.80; 0.90$ and 0.98 , were prepared on the basis of Equation (1). The two starting powders were first dry-mixed in an agate mortar, and then stirred during 5 min into petroleum ether, using an ultrasonic vibrator (Vibracell 75115 of Bioblock Scientific).

After that, the mixtures were dried at ambient temperature during 12 h, and then cold-pressed into pellets (10 mm in diameter) during 30 s under 185 MPa; finally they were sintered in pure argon (Alphagaz 1, Air Liquide, France), using a Nabertherm furnace (VHT 08/22 GR, Germany) equipped with graphite resistor. The temperature program used consisted in a ramp from ambient to 1600 °C, followed by a first hold at 1600 °C (temperature just before the melting point of titanium metal Ti, i.e. 1670 °C), during 2 h for obtaining the complete disappearing of the XRD peaks of titanium. Then, a second ramp was programmed in order to homogenize the carbide with a hold at 2100 °C during 3.5 h, and, lastly, the samples were cooled to ambient. All the ramp rates, for heating and for cooling, were set at 10 °C/min.

The post annealing treatment, in the same furnace, consisted in several successive cycles, each one being composed of a 10 h-hold at 730 °C under vacuum (ca. 0.5 Pa), preceded and followed by heating and cooling at 10 °C/min. The cumulative annealing time was noted τ .

Characterizations

The samples structures were identified by XRD with a Siemens D8 Brüker diffractometer, using the filtered $\text{Cu K}\alpha_1$ radiation, within the $2\theta = 15 - 110^\circ$ range, with steps of 0.015° and an exposure time of 1 s, in a chamber maintained thermostatically at a steady temperature of 20 °C. The X-ray patterns were indexed with the DIFFRAC + EVA software (Bruker AXS)

containing the PDF database. Peakoc software was used for the fitting of XRD patterns [12].

The densities of the sintered samples were measured by helium pycnometry (Micromeritics AccuPyc II 1340).

The samples were observed with a scanning electron microscope (Philips XL30, The Netherlands).

Electrochemical measurements were carried out at room temperature, i.e. 25 °C, in a standard three-electrode cell. An Autolab PGSTAT30 potentiostat was used, controlled by GPES and FRA 4.9 softwares (EcoChemie, Netherlands). The solution was a 1 M H_2SO_4 aqueous solution (Aldrich and Millipore MilliQ + water), deaerated by bubbling pure argon gas (Alphagaz 1, Air Liquide, France). The reference electrode was a K_2SO_4 saturated $\text{Hg}/\text{Hg}_2\text{SO}_4$ electrode and the potentials are given vs. SHE (Standard Hydrogen Electrode) by adding + 0.65 V. The counter-electrode was a platinum disk (10 mm in diameter) and the working electrode (WE) consisted in the TiC_x pellets, in a Teflon holder, with an effective surface area of 0.126 cm^2 . The WE was mounted on a rotating disk electrode system EDI 101 (Radiometer-Analytical, France) and set at a rate of 2000 rpm.

Results and discussion

Carbide structure and microstructure

Fig. 1 (a), (b) and (c) present the fracture micrographs of the sintered pieces $\text{TiC}_{0.98}$ (i.e., obtained by using the as-received titanium carbide powder), $\text{TiC}_{0.70}$ and $\text{TiC}_{0.60}$ respectively. The observed microstructures depend strongly on the stoichiometry: for the carbide $\text{TiC}_{0.98}$, the grains were small, in the range 1–5 μm , showing an incomplete sintering, with a limited grain growth and a significant intergranular porosity. This result is not surprising because the temperature used for sintering (2100 °C) is significantly lower than the melting point of $\text{TiC}_{0.98}$ (about 3160 °C), and the atomic mobility remains rather low.

For $\text{TiC}_{0.70}$, the grain growth was much higher (see Fig. 1 (b)). The grains, about 20 μm large, exhibited a noticeable porosity inter and intragranular. The grain growth was yet higher for $\text{TiC}_{0.60}$ where the grain size reached around 50 μm (Fig. 1 (c)), while the porosity was bigger and mainly located at the triple points.

The X-ray pattern of TiC_x , given in Fig. 2 (a), (b) and (c), for $\text{TiC}_{0.70}$, $\text{TiC}_{0.65}$ and $\text{TiC}_{0.55}$ respectively, confirmed that the carbide was always monophased, and the peaks were indexed with the ICDD-PDF cards n° 00-32-1383 of the cubic phase TiC (space group Fm-3m, NaCl type). Two main changes were observed when the carbon content decreases:

- a significant preferential orientation of grains, favoring the (200) planes, which was attributed to the grain growth already mentioned;
- a shift of the peaks toward the high angles, corresponding to the well known decrease of the lattice parameter together with the carbon content of the carbide [3,11]. This allowed to determine the lattice parameter, a , as a function of x , using TOPAS software.

Download English Version:

<https://daneshyari.com/en/article/1269526>

Download Persian Version:

<https://daneshyari.com/article/1269526>

[Daneshyari.com](https://daneshyari.com)